

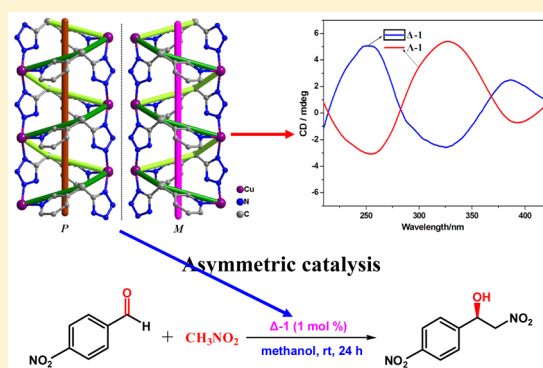
Spontaneous Resolution, Asymmetric Catalysis, and Fluorescence Properties of Δ - and Λ -[Cu(Tzmp)]_n Enantiomers from in Situ [2 + 3] Cycloaddition Synthesis

Yun-Zhi Tang,* Jian-Bo Xiong, Ji-Xing Gao, Yu-Hui Tan, Qing Xu, and He-Rui Wen

School of Metallurgy and Chemical Engineering, Jiangxi University of Science and Technology, Ganzhou 341000, Jiangxi Province, P. R. China

Supporting Information

ABSTRACT: Although a number of acentric or chiral tetrazole complexes were synthesized from Sharpless reaction, there are no spontaneous resolution Cu(I)-tetrazole compounds from in situ [2 + 3] cycloaddition synthesis that have been reported before. The first enantiomers Δ - and Λ - of metal tetrazole compound [Cu(Tzmp)]_n (**1**) (HTzmp = 3-tetrazolemethylpyridine) were obtained and isolated from in situ [2 + 3] cycloaddition reactions of a flexible organic nitrile (3-cyanomethylpyridine) with sodium azide in the presence of CuCl₂ as the Lewis acid. Δ -**1** and Λ -**1** feature a homochiral helical coordination polymeric system and {4(4).6(2)} two-dimensional framework. The photoluminescence study suggests **1** exhibits strong green fluorescence in solid state with maximal emission peaks around 535 nm. Remarkably, the Δ - and Λ - of [Cu(Tzmp)]_n (**1**) catalyzes the enantioselective Henry reaction with high yield (more than 96%) and certain enantioselectivity (up to 69%).

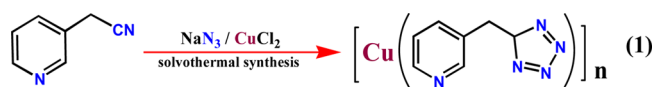


INTRODUCTION

Investigation of homochiral coordination compounds have evoked particular interest due to their wide application in asymmetric catalysis, ferroelectricity, triboluminescence, and nonlinear optical (NLO) functions (especially second harmonic generation, SHG),¹ where asymmetric catalysis and photoluminescent properties are of particular importance for their practical importance in areas such as chiral separation, telecommunications, optical storage, and information processing as well as mechanical energy transfer.² Assembling chiral metal organic frameworks (mofs) is an important avenue to obtain chiral materials and has become one of the hot topics in recent years. Nowadays, three synthetic methods have usually been used to assemble homochiral metal–organic solid materials through the protocols as follows: (a) using asymmetric, flexible, or racemic organic ligand to self-assemble with metal ion; (b) racemic organic ligand coordinating to metal ion to result in self-resolution to get chiral compounds; (c) asymmetric coordination compounds obtained through self-assembly of metal and homochiral organic ligands.³ However, the generation of homochiral solids from achiral building blocks still depends upon Edisonian (much accidental experimental) approaches, and the construction of structurally ordered chiral metal–organic solids still remains a scantily explored area.^{3h–j}

Recently, Xiong et al. have discovered a large number of acentric or chiral metal–tetrazole coordination polymers that can be obtained through Sharpless cycloaddition reaction by using organic nitrile ligands as substrate;⁴ however, most of the

organic nitrile ligand they used have grid structures such as N-4-cyanobenzylcinchonidine bromide, 3-cyano-phenylalaninate, only few chiral or acentric metal-tetrazole coordination polymers constructed from flexible organic nitrile ligands.^{4b} What's more, no spontaneous resolutions from in situ synthesis of metal tetrazole compounds have been reported. As a continuous work to seek the homochiral metal–tetrazole coordination polymers and explore their application in asymmetric catalysis, triboluminescence and nonlinear optical, we desire to design some new mofs by selecting flexible organic nitrile ligands as substrate. By this means, we fortunately obtained and isolated novel enantiomers (Δ - and Λ -) of tetrazole compound ([Cu(Tzmp)]_n, **1**) from in situ [2 + 3] cycloaddition reactions of 3-cyanomethylpyridine with sodium azide and CuCl₂ (see Scheme 1). Herein, we report the spontaneous resolution, crystal structure, circular dichroism (CD) spectra, asymmetric catalysis, and fluorescent properties of these enantiomers.

Scheme 1. Preparation of Complex **1**

Received: March 5, 2015

Published: May 13, 2015

EXPERIMENTAL SECTION

Synthesis. Hydrothermal treatment of the flexible organic ligand 3-cyanomethylpyridine (0.0236 g, 0.2 mmol), NaN₃ (0.0390 g, 0.6 mmol; **Caution! Metal azides may be explosive**), and CuCl₂ (0.0269 g, 0.2 mmol) in the presence of water (2 mL) and ethanol (0.5 mL) at 140 °C for 24 h affords the orange block crystals (Δ -1, Supporting Information, Figure S1) or needle crystals (Λ -1, Supporting Information, Figure S2) of [Cu(Tzmp)]_n (**1**). For Δ -1: Yield: 38%. For Λ -1: Yield: 37%. Anal. Calcd(%) for C₇H₆CuN₅: C, 37.68; H, 2.70; N, 31.31. Found: C, 37.72; H, 2.68; N, 31.29. Compared by the IR spectrum of ligand and sodium azide, the absence of absorptions of cyano group at 2355 cm⁻¹ $\nu_{\text{as}}(\text{C}\equiv\text{N})$ and $\nu_{\text{s}}(\text{C}\equiv\text{N})$ and azide group in 2100 cm⁻¹, while the presence of a series of new strong peaks ranges from 1613 to 1451 cm⁻¹ in title compound (Supporting Information, Figure S3) indicate that the [2 + 3] cycloaddition reaction between cyano group and azide anion have occurred.⁴

Crystallography. X-ray single-crystal diffraction data were collected on a Bruker P4 diffractometer with Mo K α radiation (λ = 0.710 73 Å) at 298 K using the θ – 2θ scan technique and corrected for Lorentz–polarization and absorption corrections.⁵ The crystal structure was solved by direct methods and refined by the full-matrix method based on F^2 by means of the SHELXLTL software package. Non-H atoms were refined anisotropically using all reflections with $I > 2\sigma(I)$. All H atoms were generated geometrically and refined using a “riding” model with Uiso = 1.2Ueq (C). The small Flack parameters for all complexes clearly indicate that the absolute structure is correctly assigned in each case.^{3f} The asymmetric units and the packing views were drawn with DIAMOND (Brandenburg and Putz, 2005). Angles between some atoms were calculated using DIAMOND, and other calculations were performed using SHELXLTL. Crystal data and structure refinement for Δ -1 and Λ -1 are listed in Table 1. Their

Table 1. Crystal Data and Structure Refinement for Δ -1 and Λ -1

compound	Δ -1	Λ -1
empirical formula	C ₇ H ₆ CuN ₅	C ₇ H ₆ CuN ₅
formula weight	223.71	223.71
temperature	298(2) K	298(2) K
crystal system	monoclinic	monoclinic
space group	$P2_1$	$P2_1$
<i>a</i> (Å)	8.3819(11)	8.3796(11)
<i>b</i> (Å)	5.7198(7)	5.7176(7)
<i>c</i> (Å)	9.3376(12)	9.3378(11)
β (deg)	115.150(3)	115.194(3)
<i>V</i> (Å ³)	405.23(9)	404.80(9)
Dcalca/M gm ⁻³	1.833	1.835
<i>Z</i>	2	2
μ (mm ⁻¹)	2.647	2.649
<i>F</i> (000)	224	224
Flack parameter	0.034(16)	0.04(2)
GOF	1.007	1.026
$R_1[I > 2\sigma(I)]$	$R_1 = 0.0224$, $wR_2 = 0.0579$	$R_1 = 0.0266$, $wR_2 = 0.0506$
wR_2 (all data)	$R_1 = 0.0248$, $wR_2 = 0.0591$	$R_1 = 0.0353$, $wR_2 = 0.0531$
$\Delta\rho_{\text{max}}/\Delta\rho_{\text{min}}$ (e Å ⁻³)	0.737/−0.205	0.692/−0.446

selected intra-atomic distances and bond angles are given in Supporting Information, Table S1. Additional crystallographic information is available in the Supporting Information.

Physical Techniques. The Fourier transform infrared spectra were recorded from KBr pellets in the range of 400–4000 cm⁻¹ on a Bruker TENSOR27 spectrometer. ¹H NMR spectra were recorded on a Varian 400 MHz spectrometer in CDCl₃ at room temperature. Powder X-ray diffraction patterns were recorded on a D8 ADVANCE diffractometer

with Cu K α radiation at a scanning rate of 4° min⁻¹ with 2θ ranging from 5° to 50°. The solid-state CD spectra were recorded on a Jasco-1500 CD spectropolarimeter at 20 °C. The CD spectra were measured on the resulting complexes as crystals (ca. 0.4 mg) in 100 mg of oven-dried KBr. The baseline correction was performed with the spectrum of a pure KBr disk. Spectra were recorded for the wavelength range of 250–700 nm, for all the disks the path length was 0.3 mm. The solid photoluminescence (PL) spectra were recorded on an Edinburgh Analytical Instruments FLS920 spectrometer.

RESULTS AND DISCUSSION

The chirality of the Δ -1 and Λ -1 enantiomers was measured by solid CD spectra that are detailed in a later section. As shown in Supporting Information, Figures S1 and S2, although Δ -1 and Λ -1 are enantiomers and crystallize in an achiral solution, they have distinctly different habits in morphology. Δ -1 tends to accumulate in the bottom of pyrex tube and feature block crystals, while Λ -1 are needle crystals and are apt to adhere on the wall of the pyrex tube or concentrate in the upper of pyrex tube. (Supporting Information, Figure S4) To our knowledge, most enantiomers that crystallize in an achiral solution have the same morphology; only a few enantiomers with different morphology have been reported, such as Δ - and Λ -[M(H₂Biim)₃]_nSO₄.^{3f}

As shown in Figure 1, both Δ -1 and Λ -1 contain one crystallographically independent [Cu(Tzmp)]_n entity with an

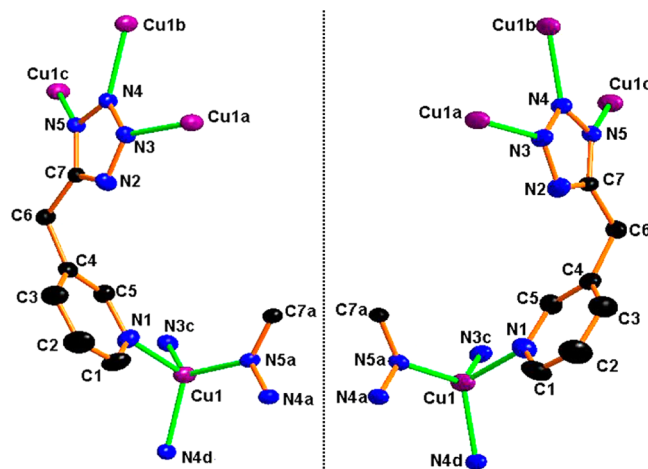


Figure 1. X-ray crystal structure show the mirror image of Δ - and Λ -[Cu(Tzmp)]_n enantiomers.

identical coordination environment, and the coordination geometry around Cu atoms in Δ -1 and Λ -1 displays perfect mirror image reflection. Here we just detailed the crystal structure of Δ -1.

Complex Δ -1 belongs to the monoclinic crystal system, with chiral space group $P2_1$ (Table 1). Remarkably, the asymmetric unit of **1** contains one Cu^I ion and one Tzmp⁻ ligand, indicating the Cu^{II} in reaction materials have been reduced to Cu^I. Most known Cu^I complexes are easy to oxidize at room temperature; however, complex **1** can be stable to 300 °C and insoluble in common organic solvents such as dimethylformamide, H₂O, MeOH, and MeCN. The central metal copper adopts four coordination modes, which are connected by two α -N, one β -N atom from three different tetrazole groups, and one N atom from the pyridyl group (Figure 2). As can be seen, all the coordinated nitrogen atoms originate from different functional groups, and thus, the copper atom can be regarded

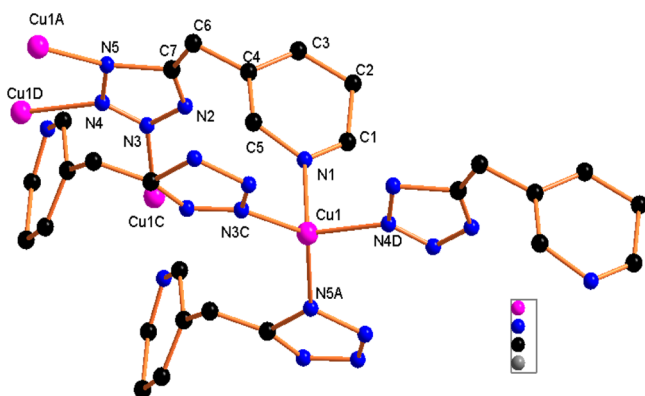


Figure 2. Asymmetric unit view of Δ -1 showing each Cu center located in highly distorted tetrahedral coordination geometry. Selected bond lengths (Å) and angles (deg): N(1)–Cu(1) 2.1343(15), Cu(1)–N(3) No. 1 1.999(2), Cu(1)–N(5) No. 3 2.005(2), Cu(1)–N(4) No. 4 2.0325(12), N(3) No. 1–Cu(1)–N(5) No. 3 125.55(5), N(3) No. 1–Cu(1)–N(4) No. 4 110.21(10), N(5) No. 3–Cu(1)–N(4) No. 4 111.60(10), N(3) No. 1–Cu(1)–N(1) 102.45(11), N(5) No. 3–Cu(1)–N(1) 98.40(10), N(4) No. 4–Cu(1)–N(1) 105.46(5). Symmetry code for Δ -1: No. 1 $-x, y + 1/2, -z$; No. 2 $-x, y - 1/2, -z$; No. 3 $x + 1, y, z + 1$; No. 4 $x - 1, y, z - 1$.

as a chiral center that is similar to the chiral carbon atoms in organic compounds. The bond length of Cu(1)–N(1) (2.135 (2) Å) is obviously longer than that of Cu(1)–N(4) No. 1 (1.997 (5) Å), Cu(1)–N(2) No. 2 (2.004 (4) Å), and Cu(1)–N(5) No. 3 (2.031(2) Å) (Supporting Information, Table S1), and all the bond angles of N–Cu–N of the tetrahedron are between 98.52(18) and 125.60(9), suggesting the central copper metal in **1** lies in a highly unsymmetrical fashion.⁶

In Δ -1, the ligand Tzmp^- is twisted with the angle of flexible C6 ($\angle\text{C4C6C7}$) of 111.058° and the dihedral angle between the tetrazole and pyridine ring of 77.952° ; the corresponding values are 110.942° and 77.810° , respectively, for Λ -1. These twisted ligands together with the metal centers conferred an infinite one-dimensional (1D) helical polymeric chain running along the crystallographic 2_1 axis in the b -direction.^{7,8} Notably, we structurally identified both right-(P) (Λ -1) and left-(M) (Δ -1) handed helices from two different crystals in the same batch, and demonstrated a case of conglomeration (Figure 3).⁷ Furthermore, because of the coordination bond of Cu1–N4 interaction, the conformation of each individual helical assembly is locked to each other, and hence the message of the homochirality is spread to a two-dimensional (2D) sheet (Supporting Information, Figure S4), which further transmitted all over the crystal by the noncovalent interactions among the homochiral layers, resulting in a homochiral self-resolution of the crystals (Figure 4).⁸ In essence, the chirality of the metal coordination units in Δ -1 and Λ -1 is induced primarily by the lock of Tzmp^- in a twisted helical environment upon coordination to a chiral metal center, assuming distorted tetrahedral geometry.⁸ To exactly describe the topological structure of compound **1**, we simplified the top structure by application of a topological approach (TOPOS software analysis).⁹ As shown in Figure 5, the net has two four-connected topologically equivalent nodes representing either Cu(I) center or an averaged ligand position, so the overall structure features an uninodal four-connected non-interpenetrated sql/Shubnikov tetragonal plane nets with $\{4(4).6(2)\}$ topology.

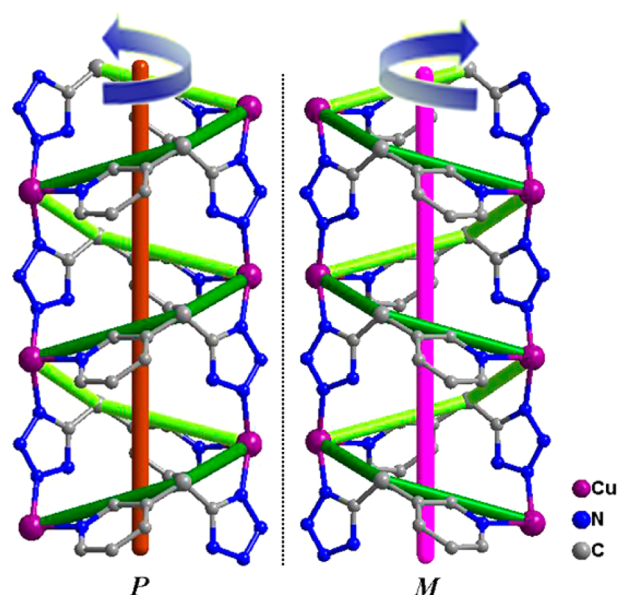


Figure 3. The P and M chiral helical structures of Δ - and Λ -1 enantiomers.

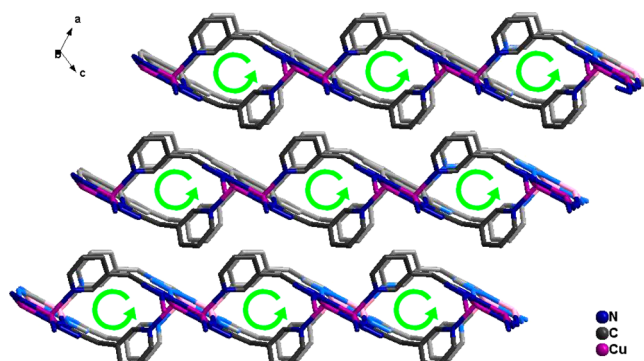


Figure 4. Homochiral assembly of the 2_1 helical chains in Δ -1 (hydrogen atoms are omitted for clarity).

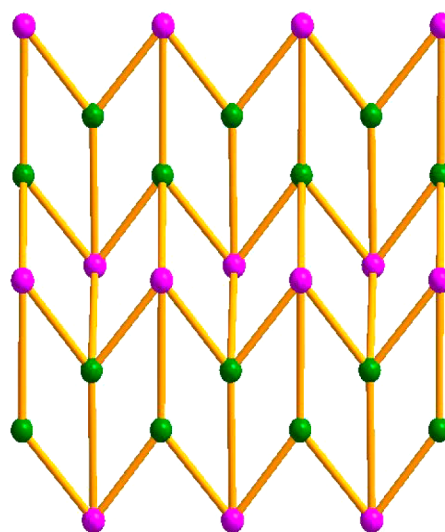


Figure 5. View of Λ -1 in the ab plane with an overlay of the $\{4(4).6(2)\}$ topology which projects a 4-c net in which the purple nodes stand for Cu atoms and the green nodes represent the simplified ligands.

To further confirm the chirality of the Δ -1 and Λ -1 enantiomers, we measured their solid CD spectra. Figure 6

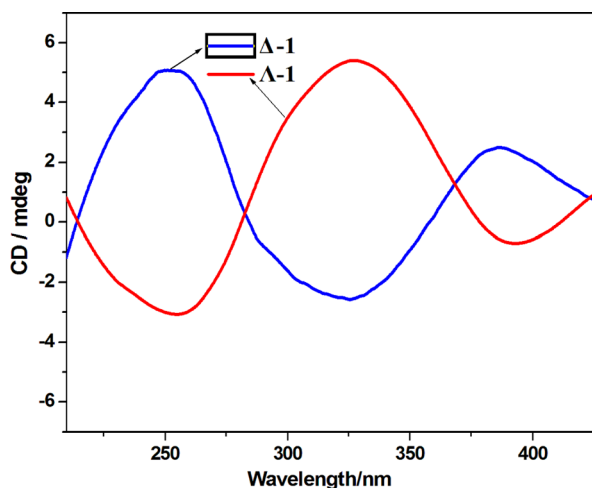


Figure 6. Circular dichroism spectra of Δ -1 (blue line) and Λ -1 (red line) in KBr pellets.

gathers the CD spectra of two different bunches. It is observed that the CD spectrum of Δ -1 exhibits a positive Cotton effect at $\lambda = 249$ and 383 nm and a negative dichroic signal centered at $\lambda = 325$ nm, while Λ -1 shows Cotton effects of the opposite sign at the same wavelengths. Moreover, we had randomly selected 15 block crystals and 15 needle crystals to perform solid-state CD spectra test; the results indicate that the block crystals always feature one kind of Cotton effect (Δ -1, blue line of the CD spectra), and the needle crystals always show the opposite Cotton effect signal (Λ -1, red line), (Supporting Information, Figure S4). These Cotton effect peaks can be assigned to the charge-transfer and d–d transitions of the UV–vis absorption spectra of these complexes, respectively.

As shown in Table 2, the transformation of the asymmetric 1-phenyl, 2-nitro-ethanol¹⁰ was examined initially by using

Table 2. Yields and Enantiomeric Excess Values of Henry Reaction Product^a

entry	catalyst	yield (%) ^b	ee (%) ^c
1	Δ -1	96	>69
2	Λ -1	96	<−69
3	1 (<i>rac</i>)	96	
4	no	37	

^aReactions were performed using 2.5 mmol of *p*-nitrobenzaldehyde, ethanol (10 mL), and nitromethane (10 equiv) by the catalysis of Δ (or Λ)-1 at room temperature. ^bThe conversions were determined by ¹H NMR spectroscopy of the crude products. ^cEnantiomeric excesses were determined by HPLC analysis on a chiral OD-H column.

benzaldehyde and nitromethane in methanol along with Δ -1 (1% mol ratio) in a heterogeneous manner at room temperature, and the product of Henry reaction was examined by ¹H NMR in CDCl₃ (Supporting Information, Figure S6). Remarkably, the Δ - and Λ - of [Cu(Tzmp)]_n (1) catalyzes the enantioselective Henry reaction (Table 2) with high yield (more than 96%). When we conducted the Henry reaction without Δ -1 (or Λ -1), the yield is only 37%. However, the result shows a commonly enantioselectivity (enantiomeric excess (ee) > 69%) for (*R*)-1-phenyl, 2-nitro-ethanol.¹¹ In

addition, the removal of ex- Δ -1 by filtration after 24 h shut down the reaction, and the filtrate afforded only 2% additional conversion after stirring at room temperature for another 24 h. These observations suggested that Δ -1 was a true heterogeneous catalyst. Solids of Δ -1 could be isolated from the reaction suspension by simple filtration alone; the powder X-ray diffraction of filter residue shows it is very highly crystalline, since their simulated PXRD pattern based on the crystal structure analysis allowed unambiguous identification via a comparison of the experimental and computed powder diffraction patterns (Supporting Information, Figure S7). In addition, the catalysts could be reused at least three times with moderate loss of activity (from 88% to 82% of yield) and a slight decrease in the selectivity (ee values from >60% to 63%). Solids of Λ -[Cu(Tzmp)]_n exhibited similar catalytic activities but gave products with opposite chiralities in the asymmetric (*S*)-1-phenyl, 2-nitro-ethanol.

As is well-known, the coordination compound containing Cu^I often shows the fluorescence property, but Cu^{II} compound does not. As we expected, solid-state of 1 exhibits a strong photoluminescence, which centered at 535 nm upon excitation at 450 nm at room temperature (Figure 7). The further

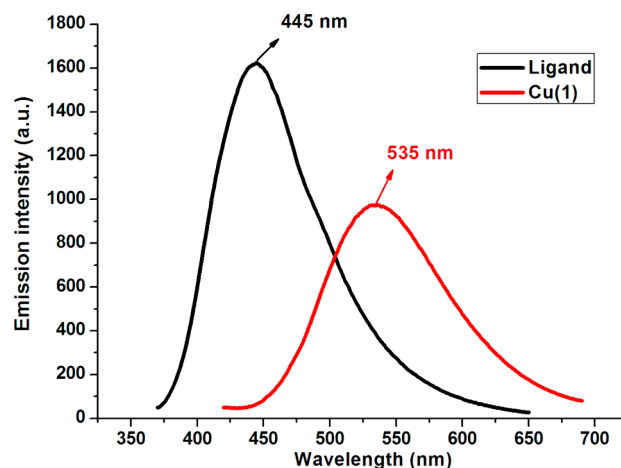


Figure 7. The solid-state fluorescent emission spectrum of 1 at room temperature.

investigation shows its lifetime and quantum yield are 3639 ns and 0.85% (Φ values), respectively, suggesting 1 may be a potential green light emitted material. According to previous research and our investigation on Cu^I–tetrazolate compounds,¹² the peaks at 535 nm may be attributed to a [Cu– π^* (tetrazolate)] metal-to-ligand charge transfer (MLCT).¹² Different from other Cu^I cluster-centered complexes such as Cu₄L₄L₄,^{12b–d} this compound presents a Cu...Cu distance of 3.590 Å at room temperature, far more than the sum of the orbital radii (2.80 Å); therefore, there is no emitting peak about Cu...Cu [3d–4s] cluster-centered (CC) excited states that was discovered. However, in light of Cotton's work through density functional theory calculations, the short Cu...Cu separation does not guarantee a metal–metal bond, and the [3d–4s] CC excited states should take into account related bonds and angles with the bridging ligands. Complex 1 exhibits a lower quantum yield (Φ) than the similar Cu^I complex such as [(CuI)₂(46dmpm)]_n, which may be attributed to the expansion of a void space from the flexible ligands increasing the vibrational excitation.

CONCLUSION

In summary, we have successfully synthesized and isolated the first Cu(I)-tetrazole enantiomers, namely, Δ - and Λ -[Cu-(Tzmp)]_n (**1**), from in situ [2 + 3] cycloaddition reactions. It seems that ligands with flexible nature and special distortion conformation are more suitable to translate chirality and form helical species, thereby constructing homochiral helical complexes successfully. Our further efforts to design and synthesize more new functional homochiral helical materials from flexible organic nitrile ligands are underway. The asymmetric catalysis and interesting fluorescence properties indicate it may have potential applications in catalytic and photoluminescent materials.

ASSOCIATED CONTENT

Supporting Information

Selected bond lengths and angles, illustration of needle crystals, IR and CD spectra, illustrated 3D supramolecular structures, NMR spectrum, powder XRD patterns, and CIF files giving crystal data, experimental details, and characterization data. CCDC reference numbers: 1036127 (Δ -**1**) and 1036128 (Λ -**1**). The Supporting Information is available free of charge on the ACS Publications website at DOI: 10.1021/acs.inorgchem.5b00478. Copies of this information may be obtained free of charge from The Director, CCDC, 12 Union Road, Cambridge, CB2 1EZ, U.K. Fax (int. code) +44(1223)336-033 or E-mail: deposit@ccdc.cam.ac.uk or <http://www.ccdc.cam.ac.uk>. CCDC No. for Δ -**1**, 1036127 and for Λ -**1**, 1036128.

AUTHOR INFORMATION

Corresponding Author

*E-mail: tangyunzhi75@163.com.

Notes

The authors declare no competing financial interest.

ACKNOWLEDGMENTS

This work was funded by the National Natural Science Foundation of China (Grant Nos. 21261009, 21471070, and 21461010), Young Scientist Foundation of Jiangxi Province and Jiangxi Province Science and Technology Support Program (20133BBE50020), the Sustentation Fund of Education Department from Jiangxi Province (GJJ13434).

REFERENCES

- (1) (a) Férey, G. *Chem. Soc. Rev.* **2008**, *37*, 191–214. (b) Liu, Y.; Xuan, W.; Cui, Y. *Adv. Mater.* **2010**, *22*, 4112–4135. (c) Yoon, M.; Srirambalaji, R.; Kim, K. *Chem. Rev.* **2012**, *112*, 1196–1231. (d) Xuan, W. M.; Zhu, C. F.; Liu, Y.; Cui, Y. *Chem. Soc. Rev.* **2012**, *41*, 1677–1695. (e) Wang, S. H.; Zheng, F. K.; Zhang, M. J.; Liu, Z. F.; Chen, J.; Xiao, Y.; Wu, A. Q.; Guo, G. C.; Huang, J. S. *Inorg. Chem.* **2013**, *52*, 10096–10104. (f) Durá, G.; Carrion, M. C.; Jalón, F. A.; Rodríguez, A. M.; Manzano, B. R. *Cryst. Growth Des.* **2013**, *13*, 3275–3282.
- (2) (a) Pilar, G. G.; Alexandre, Z.; Christophe, C.; Anne, L.; Urbano, D.; Avelino, C. *Chem. Sci.* **2013**, *4*, 2006–2012. (b) Mihalcea, I.; Zill, N.; Mereacre, V.; Anson, C. E.; Powell, A. K. *Cryst. Growth Des.* **2014**, *14*, 4729–4734. (c) Bisht, K. K.; Suresh, E. *J. Am. Chem. Soc.* **2013**, *135*, 15690–15693. (d) Liu, Q. Y.; Wang, Y. L.; Zhang, N.; Jiang, Y. L.; Wei, J. J.; Luo, F. *Cryst. Growth Des.* **2011**, *11*, 3717–3720. (e) Han, L. L.; Zhang, X. Y.; Chen, J. S.; Li, Z. H.; Sun, D. F.; Wang, X. P.; Sun, D. *Cryst. Growth Des.* **2014**, *14*, 2230–2239. (f) Sun, J. W.; Zhu, J.; Song, H. F.; Li, G. M.; Yao, X.; Yan, P. F. *Cryst. Growth Des.* **2014**, *14*, 5356–5360. (g) Kaur, A.; Hundal, G.; Hundal, M. S. *Cryst. Growth Des.* **2013**, *13*, 3996–4001.
- (3) (a) Bisht, K. K.; Suresh, E. *Inorg. Chem.* **2012**, *51*, 9577–9579. (b) Rao, A. S.; Pal, A.; Ghosh, R.; Das, S. K. *Inorg. Chem.* **2009**, *48*, 1802–1804. (c) Choi, S. W.; Ryu, D. W.; Lee, J. W.; Yoon, J. H.; Kim, H. C.; Lee, H.; Cho, B. K.; Hong, C. S. *Inorg. Chem.* **2009**, *48*, 9066–9068. (d) Low, Y. Y.; Gan, C. Y.; Kam, T. S. *J. Nat. Prod.* **2014**, *77*, 1532–1535. (e) Lennartson, A.; Hedström, A.; Hakansson, M. *Organometallics* **2010**, *29*, 177–183. (f) Tan, Y. H.; Wu, J. J.; Zhou, H. Y.; Yang, L. F.; Ye, B. H. *CrystEngComm* **2012**, *14*, 8117–8123. (g) Duan, X. Y.; Meng, Q. J.; Su, Y.; Li, Y. Z.; Duan, C. Y.; Ren, X. M.; Lu, C. S. *Chem.—Eur. J.* **2011**, *17*, 9936–9943. (h) Hang, T.; Fu, D.-W.; Ye, Q.; Xiong, R.-G. *Cryst. Growth Des.* **2009**, *9*, 2026–2029. (i) Bisht, K. K.; Suresh, E. *J. Am. Chem. Soc.* **2013**, *135*, 15690–15693. (j) Morris, R. E.; Bu, X. *Nat. Chem.* **2010**, *2*, 353–361.
- (4) (a) Zhao, H.; Qu, Z. R.; Ye, H. Y.; Xiong, R. G. *Chem. Soc. Rev.* **2008**, *37*, 84–100. (b) Wang, S. H.; Zheng, F. K.; Zhang, M. J.; Liu, Z. F.; Chen, J.; Xiao, Y.; Wu, A. Q.; Guo, G. C.; Huang, J. S. *Inorg. Chem.* **2013**, *52*, 10096–10104.
- (5) (a) Sheldrick, G. M. *SHELXS-97, Program for X-ray Crystal Structure Refinement*; University of Göttingen: Germany, 1997, 208. (b) Sheldrick, G. M. *SHELXS-97, Programs zur Lösung von Kristallstrukturen*; University of Göttingen: Germany, 1997, 509.
- (6) (a) Tang, Y. Z.; Zhou, M.; Wen, H. R.; Cao, Z.; Wang, X. W.; Huang, S. *CrystEngComm* **2011**, *13*, 3040–3045. (b) Tang, Y. Z.; Zhou, M.; Huang, J.; Tan, Y. H.; Wu, J. S.; Wen, H. R. *Inorg. Chem.* **2013**, *52*, 1679–1681.
- (7) (a) Dong, L. J.; Chu, W.; Zhu, Q. L.; Huang, R. D. *Cryst. Growth Des.* **2011**, *11*, 93–99. (b) Lluisa, P. G.; David, B. A. *Chem. Soc. Rev.* **2007**, *36*, 941–967. (c) Zhang, J. P.; Lin, Y. Y.; Huang, X. C.; Chen, X. M. *Chem. Commun.* **2005**, 1258–1260.
- (8) (a) Huang, Y. G.; Mu, B.; Schoenecker, P. M.; Carson, C. G.; Karra, J. R.; Cai, Y.; Walton, K. S. *Angew. Chem., Int. Ed.* **2011**, *50*, 436–440. (b) Chen, X. D.; Du, M.; Mak, T. C. W. *Chem. Commun.* **2005**, 4417–4419. (c) Balamurugan, V.; Mukherjee, R. *CrystEngComm* **2005**, *7* (54), 337–341.
- (9) (a) Blatov, V. A.; O'Keeffe, M.; Proserpio, D. M. *CrystEngComm* **2010**, *12*, 44–48. (b) O'Keeffe, M.; Peskov, M. A.; Ramsden, S. J.; Yaghi, O. M. *Acc. Chem. Res.* **2008**, *41*, 1782–1789. (c) Alexandrov, E. V.; Blatov, V. A.; Kochetkov, A. V.; Proserpio, D. M. *CrystEngComm* **2011**, *13*, 3947–3958. (d) Blatov, V. A.; Proserpio, D. M. In *Modern Methods of Crystal Structure Prediction*; Oganov, A. R., Ed.; Wiley-VCH: Weinheim, Germany, 2011; Vol. 1, pp 1–28.
- (10) (a) Novitchi, G.; Pilet, G.; Ungur, L.; Moshchalkov, V. V.; Wernsdorfer, W.; Chibotaru, L. F.; Luneau, D.; Powell, A. K. *Chem. Sci.* **2012**, *3*, 1169–1176. (b) Shen, K.; Liu, X. H.; Wang, W. T.; Wang, G.; Cao, W. D.; Li, W.; Hu, X. L.; Lin, L. L.; Feng, X. M. *Chem. Sci.* **2010**, *1*, 590–595. (c) Jin, W.; Li, X.; Wan, B. *J. Org. Chem.* **2011**, *76*, 484–491.
- (11) (a) Wu, P. Y.; He, C.; Wang, J.; Peng, X. J.; Li, X. Z.; An, Y. L.; Duan, C. Y. *J. Am. Chem. Soc.* **2012**, *134*, 14991–14999. (b) Han, Q. X.; He, C.; Zhao, M.; Qi, B.; Niu, J. Y.; Duan, C. Y. *J. Am. Chem. Soc.* **2013**, *135*, 10186–10189. (c) Wang, X. S.; Chrzanowski, M.; Yuan, D. Q.; Sweeting, B. S.; Ma, S. Q. *Chem. Mater.* **2014**, *26*, 1639–1644.
- (12) (a) Tang, Y. Z.; Wang, G. X.; Ye, Q.; Xiong, R. G.; Yuan, R. X. *Cryst. Growth Des.* **2007**, *7*, 2382–2386. (b) Wittenberger, S. J.; Donner, B. G. *J. Org. Chem.* **1993**, *58*, 4139–4141. (c) Maini, L.; Braga, D.; Mazzeo, P. P.; Ventura, B. *Dalton Trans.* **2012**, *41*, 531–539. (d) Kitada, N.; Ishida, T. *CrystEngComm* **2014**, *16*, 8035–8040.